Oncogene (2014), 1–10

www.nature.com/onc

ORIGINAL ARTICLE

TAZ is required for metastatic activity and chemoresistance of breast cancer stem cells

M Bartucci[1,7], R Dattilo[1,7], C Moriconi[1], A Pagliuca[1], M Mottolese[2], G Federici[2], A Di Benedetto[2], M Todaro[3], G Stassi[3], F Sperati[2], MI Amabile[4], E Pilozzi[5], M Patrizii[1], M Biffoni[1], M Maugeri-Saccà[2], S Piccolo[6] and R De Maria[2]

Metastatic growth in breast cancer (BC) has been proposed as an exclusive property of cancer stem cells (CSCs). However, formal proof of their identity as cells of origin of recurrences at distant sites and the molecular events that may contribute to tumor cell dissemination and metastasis development are yet to be elucidated. In this study, we analyzed a set of patient-derived breast cancer stem cell (BCSC) lines. We found that *in vitro* BCSCs exhibit a higher chemoresistance and migratory potential when compared with differentiated, nontumorigenic, breast cancer cells (dBCCs). By developing an *in vivo* metastatic model simulating the disease of patients with early BC, we observed that BCSCs is the only cell population endowed with metastatic potential. Gene-expression profile studies comparing metastagenic and non-metastagenic cells identified TAZ, a transducer of the Hippo pathway and biomechanical cues, as a central mediator of BCSCs metastatic ability involved in their chemoresistance and tumorigenic potential. Overexpression of TAZ in low-expressing dBCCs induced cell transformation and conferred tumorigenicity and migratory activity. Conversely, loss of TAZ in BCSCs severely impaired metastatic colonization and chemoresistance. In clinical data from 99 BC patients, high expression levels of TAZ were associated with shorter disease-free survival in multivariate analysis, thus indicating that TAZ may represent a novel independent negative prognostic factor. Overall, this study designates TAZ as a novel biomarker and a possible therapeutic target for BC.

Oncogene advance online publication, 17 February 2014; doi:10.1038/onc.2014.5

Keywords: breast cancer; cancer stem cells; chemotherapy; TAZ; metastasis

INTRODUCTION

Breast cancer (BC) is a major public health concern with more than a million new cases diagnosed annually worldwide.[1] Metastatic growth in distant sites is the predominant cause of death in BC patients. Growing evidences indicate that a cellular subpopulation with stem cell (SC)-like features, known as cancer SCs (CSCs), is critical for tumor generation and maintenance.[2–6] In addition, CSCs have been recently suggested to be responsible for BC metastasis.[7,8] Indeed, it is conceivable that several of the traits ascribed to CSCs may provide them with the potential to occupy and prosper at distant sites. Yet, a functional proof of this notion is currently lacking. To progress in this direction, it is important to define, at the molecular level, players and mechanisms conferring metastatic behavior to CSCs. Here we compared a set of patient-derived breast cancer SC (BCSC) lines with their differentiated breast cancer cell (dBCC) progeny.

We found that *in vitro* BCSCs display enhanced chemoresistance and migratory capacity than dBCCs. More importantly, by developing an *in vivo* metastatic model simulating the natural course of early BC, we confirmed the exclusive ability of BCSCs to migrate and grow at secondary sites when compared with dBCCs. By molecular profiling, we identified the Hippo transducer TAZ as significantly upregulated in metastatic lesions from primary BC cells. TAZ is involved in enhanced cell proliferation, migration and transformation.[9] Critically, for the present study, TAZ has been previously shown to serve as a key CSC determinant in BC.[10] Intriguingly, TAZ is induced by and mediates the effects of epithelial-to-mesenchymal-transition, a complex cellular program well known for its association to epithelial plasticity and BC stemness.[10,11] However, the roles of TAZ-induced CSC potentials in primary BC metastasis and chemoresistance have not been explored. In this study, we provide evidence that TAZ is required for the metastatic ability and chemoresistance of BCSCs. Moreover, we show that TAZ represents a novel independent negative prognostic factor in BC. Targeting TAZ and cognate downstream signaling effectors may therefore have clinical utility for cancer therapy.

RESULTS

Characterization and validation of breast cancer stem cells (BCSCs)

Starting from primary invasive breast carcinomas (Supplementary Table S1), we isolated and characterized cells bearing SC properties. The relative abundance of $CD44^+/CD24^{-/low}$ cells in BC has an average of 6.12%.[12] Thus, following tumor sample dissociation, cell suspensions were maintained in specific culture conditions that allowed the expansion of undifferentiated cancer stem and progenitor cells, while negatively selecting serum-dependent tumor and non-transformed accessory cells.[13–15] These cell cultures were essentially composed of the so-called tumor

[1]Department of Hematology, Oncology and Molecular Medicine, Istituto Superiore di Sanità, Rome, Italy; [2]Regina Elena National Cancer Institute, Rome, Italy; [3]Department of Surgical and Oncological Sciences, University of Palermo, Palermo, Italy; [4]Department of Surgical Sciences, 'La Sapienza' University, Rome, Italy; [5]Department of Clinical and Molecular Medicine, Sant'Andrea Hospital, 'La Sapienza' University, Rome, Italy and [6]Department of Histology, Microbiology and Medical Biotechnologies, University of Padua School of Medicine, Padua, Italy. Correspondence: Dr M Bartucci, Department of Hematology, Oncology and Molecular Medicine, Istituto Superiore di Sanità, Rome 00161, Italy. E-mail: monicabartucci@yahoo.com

[7]These authors contributed equally to this work.

Received 24 July 2013; revised 3 December 2013; accepted 24 December 2013

'mammospheres' (Figure 1a) formed by a majority of $CD44^{+}/CD24^{-/low}$ cells, excluding the BCSC#3 cell line highly positive for the $CD44^{+}CD24^{+}$ profile (Supplementary Figure 1a). BCSCs fail to express the lineage-specific markers of two mammary epithelium compartments, basal cytokeratin 14 (CK14) and luminal cytokeratin 18 (CK18)[15] (Supplementary Figure 1b). To determine the *in vitro* differentiation potential of our patient-derived BCSC lines, BC spheres were dissociated and grown on collagen. Subsequently, cells were covered with matrigel, a culture technique documented to be more efficient in inducing differentiation of progenitor cells in cultures.[16,17] Under such conditions cells acquired the typical epithelial-like morphological features (Figure 1b, left panel). Additionally, exposure to this differentiation setting resulted in a marked reduction of the clonogenic growth of these cells in agar, as compared with BCSCs (Figure 1b, right panel). Consistently, matrigel-differentiated cells expressed either the basal epithelial marker smooth muscle actin or the luminal epithelial marker CK 8/18 (Supplementary Figure 1c). These results revealed that our BC spheres are composed by undifferentiated cells able to expand in the presence of opportune growth factors but, under proper conditions, readily generating differentiated BC cells (dBCCs) resembling the main cellular populations of the

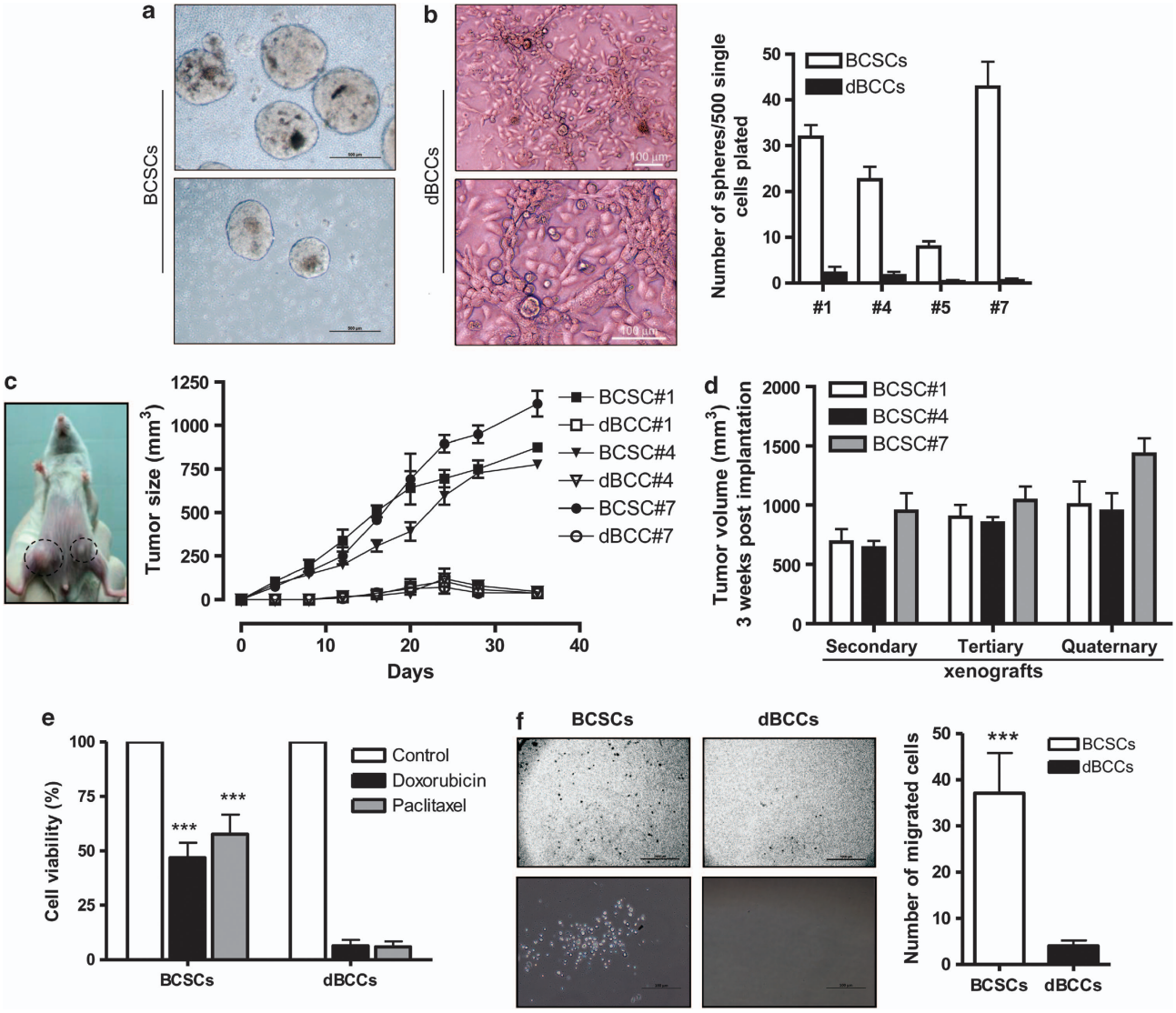

Figure 1. BCSCs are tumorigenic, chemoresistant and migrate more compared with dBCCs. (**a**) Descriptive pictures of primary human BCSCs morphology cultured in serum-free conditions (scale bars, 500 μm). (**b**) Left panel: descriptive images of dBCCs after 3 weeks of culture (scale bars, 100 μm). Right panel: self-renewal ability of BCSCs vs dBCCs. Mean ± s.d. of three independent experiments is shown. (**c**) Left panel: representative image showing tumorigenic potential of 5×10^4 BCSCs (left) as compared with 5×10^4 dBCCs. Cells were simultaneously injected into the right and left flank of the same mouse and picture was taken at day 25 after cell injection. Right panel: tumor growth rate kinetics of xenografts generated following orthotopic injection of BCSC#1, BCSC#4 and BCSC#7 and differentiated counterparts. Three mice/group were employed. (**d**) Tumorigenic potential of BCSC#1, BCSC#4 and BCSC#7-derived xenografts assessed by injecting 5×10^4 cells into mammary fat pad (secondary xenografts), BCSC spheres derived by such secondary xenografts (tertiary xenografts) and BCSC spheres derived by tertiary xenografts (quaternary xenografts). Data are mean ± s.d. of two different experiments. (**e**) Cell viability of treated and untreated (control) BCSCs and corresponding differentiated progeny. Doxorubicin (15 ng/ml) and paclitaxel (5 ng/ml) were added for 48 h and cell viability was subsequently measured by CellTiter-Glo assay. (**f**) Left: illustrative pictures of BCSCs and dBCCs migration capacity. Cell motility was assessed after 24-h incubation in modified boyden chambers and in serum-free media (scale bars, 1000 μm and 100 μm). Right: graph showing the number of migrated cells in standard growth conditions. Both the results shown in (**e** and **f**) are the mean ± s.d. of three independent experiments performed by using four different BCSC and dBCC lines.

breast epithelium. Liquid culture sphere formation analysis revealed that 12–24% of cells in mammospheres could be expanded for a number of passages while maintaining tumorigenic activity (Supplementary Figure 2). To directly compare the tumorigenic potential of the two cell populations, we injected an increasing number of BCSCs and dBCCs into the left and right mammary fat pad of immunodeficient mice, respectively. Xenotransplantation of BCSCs resulted in the formation of palpable tumors within 3–6 weeks, even when as low as 10^3 cells were injected (Supplementary Figure 3). While BCSCs were highly tumorigenic and originated tumors with stable exponential growth, dBCCs generated tumors at a very low frequency and only when injected at a high number (Supplementary Figure 3). Moreover, such dBCC-xenografts were barely able to increase in size for ~3–4 weeks before declining (Figure 1c, right and left panel). It is important to note that , BCSCs-derived xenograft cells could be serially transplanted in secondary and tertiary recipients (Figure 1d).

BCSCs are chemoresistant and possess higher migratory capacity *in vitro*

To evaluate CSCs involvement in BC progression, we investigated chemoresistance and migration capability of patient-derived BCSCs before and after differentiation *in vitro*. BCSCs and dBCCs were exposed to paclitaxel and doxorubicin, two of the most commonly used chemotherapeutic drugs in BC. Cell viability assay confirmed a more pronounced drug-induced cytotoxicity in dBCCs when compared with BCSCs (Figure 1e). Additionally, we assessed the 'basal' aptitude of BCSCs and differentiated progeny to migrate in modified Boyden chambers. We found that BCSCs not only possess a higher migratory capacity than dBCCs, but are also moderately capable to pass across the polycarbonate membrane and occupy the lower chamber, thus proving their ability to invade as well. Conversely, dBCCs migratory potential was almost undetectable (Figure 1f, left and right panel).

Only BCSCs exhibit metastatic ability *in vivo*

To overcome the limits of *in vitro* models and to better understand metastasis development *in vivo*, we pursued two different strategies in mice, both relying on the delivery of combined or single population of engineered BCSCs and dBCCs. Matched BCSC lines and dBCCs were differentially transduced with lentiviral vectors encoding either luciferase/enhanced green fluorescent protein (Luc/EGFP-BCSCs) or luciferase/red fluorescent protein (Luc/RFP-dBCCs) reporter genes. Initially, the metastatic rate of BCSCs and dBCCs was determined upon intracardiac injection. This approach allows the systemic distribution of the cell populations to all organs for the analysis of organ-specific extravasation, survival in the newly invaded site and retention of tumor-forming capacity. Mice were inoculated with Luc/EGFP-BCSCs and Luc/RFP-dBCCs, alone or combined at the defined ratio of 1:1 (Figure 2a). The appearance of metastatic lesions was then followed by bioluminescence detection with an *in vivo* imaging system. Bioluminescence signals became evident only in BCSCs-injected mice, alone or combined with Luc/RFP-dBCCs (Supplementary Figure 4a). Following target organ explants (lungs,

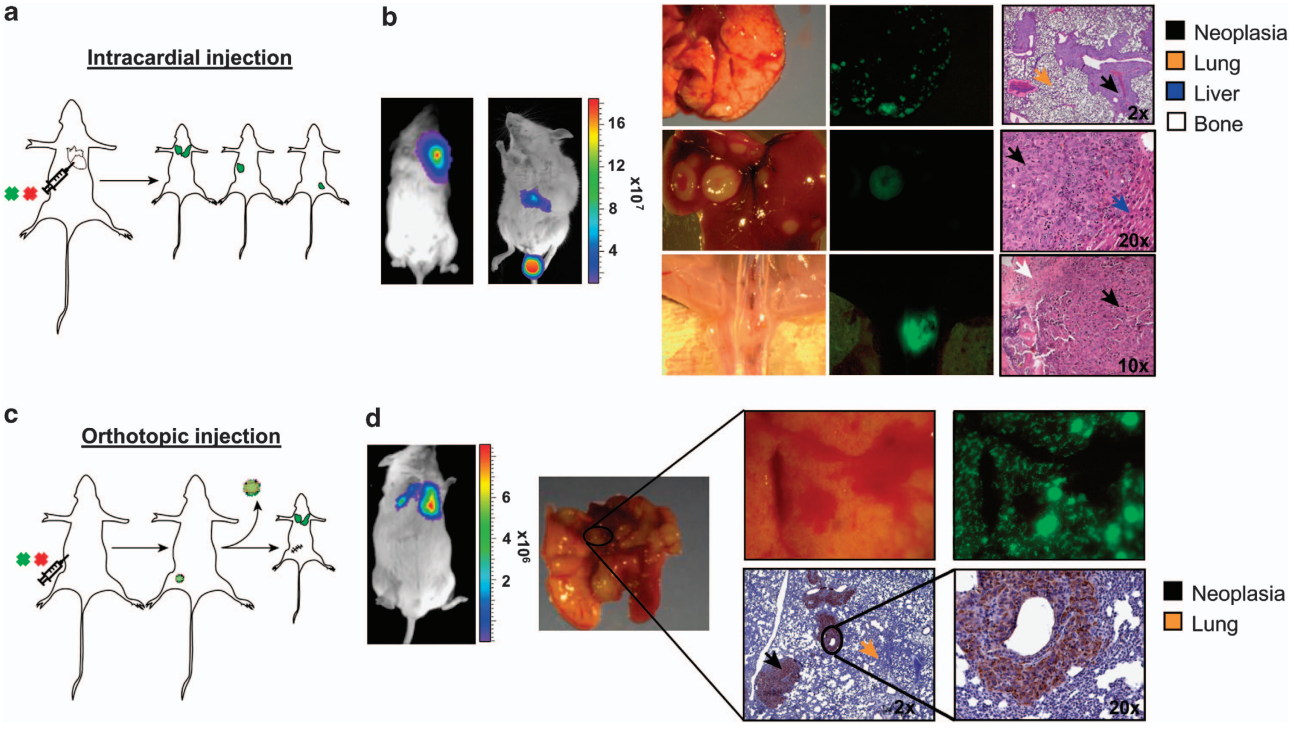

Figure 2. Assessment of metastatic *in vivo* models and migratory potential of BCSCs. (**a**) Schematic representation of intracardiac/metastatic model. Matched BCSC lines and dBCCs were differentially transduced with lentiviral vectors encoding either luciferase/enhanced green fluorescent protein (Luc/EGFP-BCSCs) or luciferase/red fluorescent protein (Luc/RFP-dBCCs) reporter genes injected alone or combined at a defined ratio of 1:1. (**b**) Left: image of a tumor metastasis monitored by bioluminescence imaging (BLI). Right: transmitted-light, fluorescent stereomicroscopic pictures and H&E staining indicating BC metastasis (black arrows) to the lung (yellow arrow), liver (blue arrow) and to the bone (white arrow) of NSG mice. (**c**) Schematic representation of orthotopic/metastatic model. Luc/EGFP-BCSCs and Luc/RFP-dBCCs were orthotopically injected at a defined ratio of 1:1. After reaching a volume of ~300 mm^3, primary tumors were removed and appearance of metastases monitored in time. (**d**) Left: representative BLI of animals showing lung metastases at day 49 after cell injection. Right: transmitted-light and fluorescent stereomicroscopic pictures of Luc/EGFP-BCSC-derived lung metastases. Immunohistochemistry was performed on formalin-fixed, paraffin-embedded tissues stained with PanCKs, highlighting the presence of neoplastic cells (black arrow) in the lung of the mouse (yellow arrow). In all BLI images, the color scale depicts the photon flux (photons per second) emitted.

liver, bones), stereomicroscopical evaluation detected the presence of green fluorescent spots, indicating that BCSCs represent the only population able to generate secondary lesions (Figure 2b). Nevertheless, it must be taken into consideration that the metastatic process encompasses a series of steps in which cancer cells leave the primary site of origin in order to colonize distant organs. Therefore, we created a more 'translational' *in vivo* model. The primary tumor was obtained by the orthotopic injection of differentially labeled BCSCs and dBCCs (1:1 ratio). Then, to mimic a radical surgical procedure, the tumor was resected and the onset of metastasis monitored (Figure 2c). Even on orthotopic injection followed by tumor resection, the only population capable to generate distant metastases was Luc/EGFP-BCSCs, as highlighted by the presence of green fluorescent foci (Figure 2d). Immunofluorescence analysis performed on labeled BCSCs/dBCCs-derived xenografts revealed that both round and elongated tubular-like arrangements spotted inside the tumor mass were entirely formed by Luc/EGFP-BCSCs, which invaded equally the ducts and the surrounding tissues (Supplementary Figure 4b). By contrast, Luc/RFP-dBCCs were chaotically distributed and unable to recreate the mammary tubulo-alveolar structures. Overall, the development of this *in vivo* metastatic model enabled us to validate the preferential ability of patient-derived BCSCs to migrate and grow at distant sites when compared with dBCCs.

Molecular profiling of BCSCs/dBCCs-derived primary and metastatic tumors revealed TAZ as a mediator of BCSCs metastasis

Given the differential metastatic ability documented after *in vivo* experiments between dBCCs and BCSCs, we searched for genes potentially responsible for this particular different biological behavior. To avoid possible biases deriving from *in vitro* culture conditions, we generated primary xenografts and subsequent metastases by injecting the two populations of undifferentiated and differentiated BC cells into the humanized fat pad. dBCCs, BCSCs and metastatic BCCs, thereafter referred to as fat pad differentiated cells (FPD), fat pad stem cells (FPS) and lung metastases (LMs), respectively, were consequently isolated from primary and metastatic lesions through fluorescent-activated cell sorting (Supplementary Figure 5a). A comparative genome-wide expression study revealed ~160 genes differentially expressed in a pool of the three populations (Supplementary Table S2). To prioritize these candidate genes and associate their expression with the metastatic proclivity of BCSCs *in vivo*, we screened for genes whose expression in BC was associated with CSCs traits, focusing on those whose upregulation level followed the rank: FPS > FPD between the first 20 differentially regulated ones (Figure 3a and Supplementary Table S2). This 'priority categorization' provided the rationale to explore the role of WWTR1, also known as the Hippo pathway transducer TAZ, in BCSCs metastases. This attracted our attention, as TAZ had recently been shown to induce self-renewal and tumor initiation capacities of BC stem-like cells derived from immortalized cell lines.[10] Similar to gene expression profiling, western blot analyses confirmed that TAZ protein levels were higher in LM cells than in FPS, whereas in FPD it was only weakly expressed (Figure 3b). In line with this, analysis of TAZ expression between distinct primary and metastatic xenografts revealed that TAZ expression levels were always considerably higher in tumor metastases (Supplementary Figure 5b). Moreover, because TAZ activity correlates with nuclear localization,[18] we analyzed several FPS and FPD and found that TAZ was barely expressed and predominantly cytoplasmic in FPD, whereas it was abundant and nuclear in FPS (Figure 3c), thus indicating that TAZ is predominantly active in the metastagenic cell compartment of a tumor. Consistently, increased levels of TAZ were associated with increased levels of CTGF and Survivin (Supplementary Figure 5c), known to be its target genes and to have an important role in tumorigenesis.[19,20]

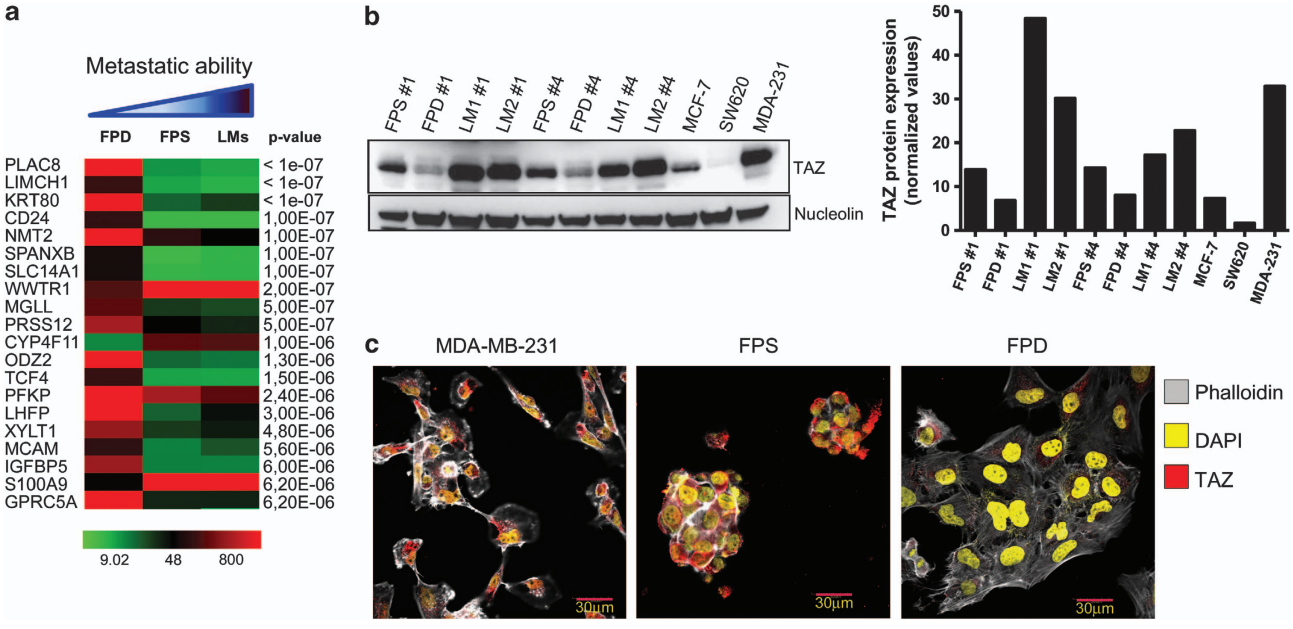

Figure 3. Gene expression profiling reveals TAZ as molecular candidate involved in BCSCs metastatic proclivity. (**a**) Hierarchical clustering of statistically differentially expressed genes in fat pad stem (FPS), fat pad differentiated (FPD) and lung metastasis (LMs) cells derived from orthotopic injection of two different BCSC lines and differentiated counterparts. Distinct cell populations were isolated from primary and metastatic tumors through fluorescent-activated cell sorting. Each column represents the average of three biological replicates. Color scale indicates the relative signal intensity. (**b**) Left: TAZ expression levels in FPS, FPD and LMs derived from the orthotopic injection of BCSCs and dBCCs #1 and BCSCs and dBCCs #4. MCF-7, MDA-MB-231 and SW620 were employed as positive and negative controls. The relative densitometric values were normalized over nucleolin, used as loading control (Right panel). A representative of three independent experiments is shown. (**c**) Representative immunofluorescent staining on FPS and FPD for TAZ expression and localization. Cells were stained with phalloidin and DAPI to visualize cell membrane and nuclei. Scale bar, 30 μm.

TAZ contributes to BCSCs chemoresistance

Resistance to DNA damage-induced apoptosis, motility, invasiveness and clonogenicity are relevant in the metastatic process.[21] BC generally responds to therapy at the beginning of treatment, but such responsiveness progressively decreases following multiple therapeutic regimens.[22,23] TAZ has been correlated with drug resistance in BC cell lines.[10,24] Accordingly, metastasis-derived cells (TAZ overexpressing cells) resulted more resistant to chemotherapy than the primary tumor-derived cells (LMs > FPS > FPD) (Figure 4a). To assess the role of TAZ in BCSC chemoresistance, we performed loss-of-function analyses of TAZ in BCSCs (Figure 4b and Supplementary Figure 6a). Cell viability assay revealed that BCSCs controls (BCSCs LKO NT and super GFP) were considerably more resistant to both paclitaxel- and doxorubicin-induced cell death than TAZ-depleted cells (BCSCs LKO shTAZ, shTAZ1 and shTAZ3) (Figure 4c and Supplementary Figure 6b). Concomitantly, we assessed gain-of-function analyses of TAZ in dBCCs. In contrast, we observed that overexpression of TAZ in dBCCs (dBCCs TWEEN TAZ) was not sufficient to significantly counteract chemotherapy-induced cell death (Figure 4c). Likewise, we evaluated the effect of doxorubicin on human BC xenografts generated by transplantation of BCSCs LKO NT and BCSCs LKO shTAZ into NSG mice. Remarkably, silencing of TAZ enhances the efficacy of chemotherapy *in vivo* (Figure 4d and Supplementary Figure 7), thus suggesting that TAZ contributes to drug resistance in BC.

TAZ supports tumorigenic potential and determines metastasis-promoting capabilities of BCSCs

To evaluate TAZ involvement in the tumor-seeding ability and metastatic potential of BCSCs and dBCCs, we compared tumorigenic capacity of BCSCs LKO shTAZ, dBCCs TWEEN TAZ with their respective controls (BCSCs LKO NT and dBCCs TWEEN) in immunodeficient mice. Knocking down TAZ protein levels altered the growth of primary BCSC-derived tumors when a non-saturating, low number of cells (50–500), was injected (Figure 5a). Consequently, we observed that on TAZ overexpression, dBCCs developed a more spindle-shaped-like appearance *in vitro* (Figure 5b) and totally reverted their tumorigenic capacity *in vivo* (Figure 5c). Thus, TAZ has a role in the seeding ability of tumor cells. Crucially, silencing TAZ expression in BCSCs hampered cell motility *in vitro* (Figure 5d) and reverted metastasis onset *in vivo,* even when up to 5×10^4 cells/group were injected (Figure 5e). Accordingly, the motility of TAZ-overexpressing dBCCs was dramatically enhanced *in vitro* (approximately fivefold) and their metastatic ability considerably increased *in vivo* (Figures 5d and e).

TAZ protein is overexpressed in BC metastases

The finding that TAZ was intensely overexpressed in BCSCs-derived metastases as well as having a critical role in cell migration and invasion, prompted us to investigate TAZ levels in metastatic lesions from human BCs. We selected 56 primary BCs (PBCs) with their paired metachronous metastases. We found that among the 19 TAZ-negative PBCs, only 6 (32%) maintained a concordant score in the matched metastases, whereas 13 (68%) displayed an increased TAZ expression level starting from score 1 + (26%), 2 + (32%) and 3 + (10%). Likewise, among the 16 PBCs with a score of 1 + and the 17 with a score of 2 +, we observed an increase in TAZ expression in 15 out of 33 (45%) paired metastases, whereas TAZ expression was lost only in 1 metastatic lesion derived from a score of 2 + PBC (Figure 6a and Table 1). Moreover, the analysis of BCSC-derived xenografts showed a clear increase in TAZ expression in tumor metastases as compared with the paired primary lesions (Supplementary Figure 5b), thus confirming the tendency of TAZ to increase in the metastatic site.

TAZ is an independent prognostic marker in BC

Recently, analyses of BC patients gene-expression data sets correlated TAZ activity with histological grading and higher probability to develop metastases.[10] However, it is unknown

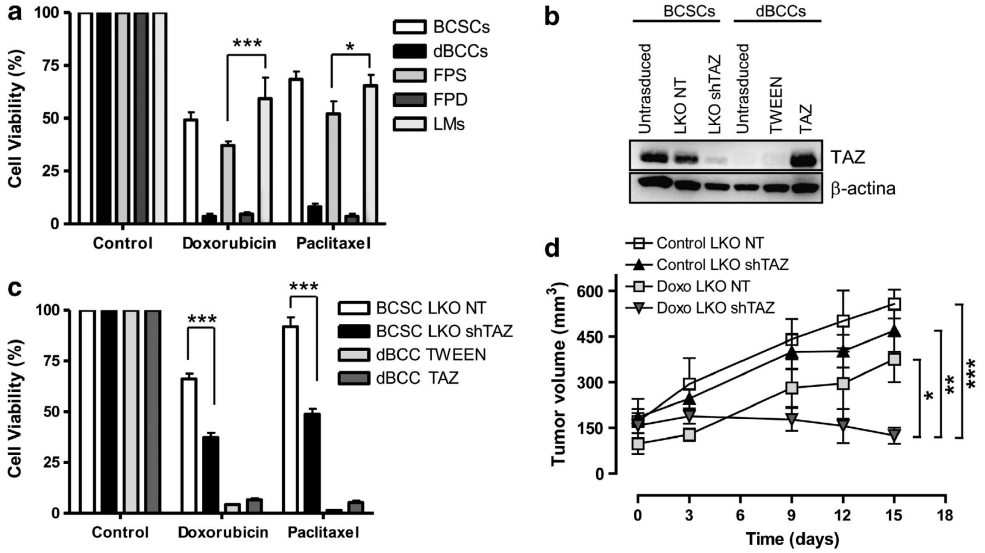

Figure 4. TAZ is involved in BCSCs chemoresistance. (**a**) Cell viability of BCSCs, dBCCs and corresponding FPS, FPD and LMs on chemotherapy treatment. Experiments performed starting from three different BCSC lines are shown. (**b**) Western blot analysis for TAZ expression in cell lysates from untransduced BCSCs and dBCCs, control vector-transduced (LKO NT and TWEEN), TAZ-depleted (LKO shTAZ) and TAZ-overexpressing (TWEEN TAZ) cells. β-actin was used to assess equal loading. (**c**) Chemosensibility evaluated on control vector-transduced (BCSC LKO NT and dBCC TWEEN), TAZ-depleted BCSC LKO shTAZ and TAZ-overexpressing dBCC TWEEN TAZ. (**d**) Growth rate of mouse xenografts generated after orthotopic injection of 5×10^4 BCSC LKO NT, BCSC LKO shTAZ untreated and treated with doxorubicin (2 mg/kg). Results are mean ± s.d. of two independent experiments. In the results shown in panels **a** and **c**, paclitaxel was used at 5 ng/ml and doxorubicin at 15 ng/ml. Cells were treated for 48 h and viability was measured by CellTiter-Glo assay. Both are the mean ± s.d. of three independent experiments.

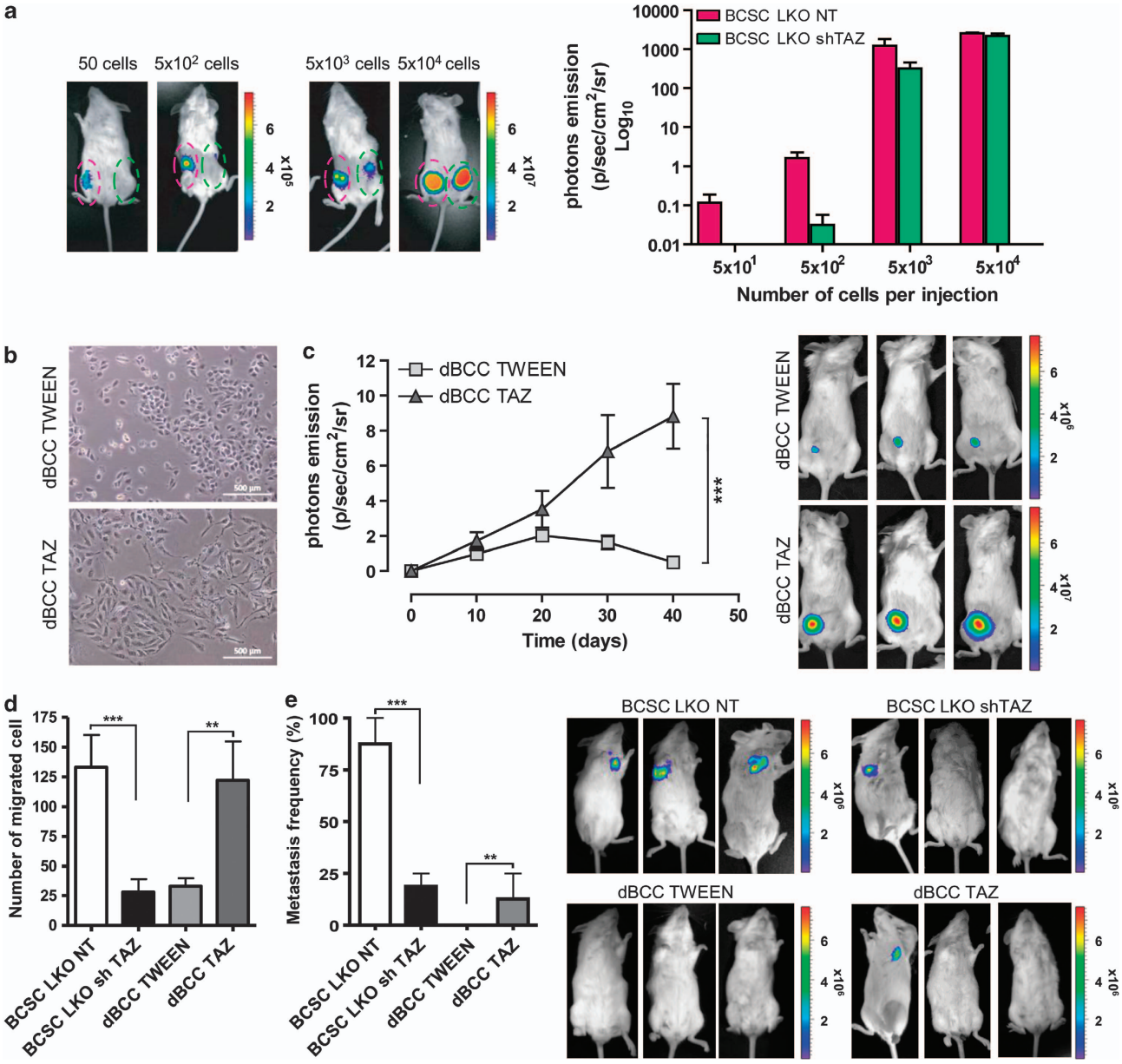

Figure 5. TAZ supports self-renewal capacity and is required for BCSC migration. (**a**) Tumor-seeding ability of control BCSCs LKO NT and TAZ-depleted BCSCs LKO shTAZ. The indicated number of cells was orthotopically injected into NSG mice. Left image is representative of tumor growth monitored by BLI with the color scale depicting the photon flux emitted. Right panel shows a graphical representation of cell-related tumor growth. Results shown are the mean ± s.d. of three experiments performed with groups of three mice each. (**b**) Representative image showing morphologic changes in dBCCs following TAZ overexpression. Cell morphology was examined by phase contrast microscopy. (**c**) Left: tumor growth curves related to the tumor-seeding ability of dBCCs TWEEN and dBCCs TWEEN TAZ. For each cell population, 5×10^4 cells were injected into the fat pads of NSG mice. Data are the mean ± s.d. of three independent experiments in which three mice/group were employed. Right: representative BLI image at day 30 post cells implantation indicating the tumorigenic potential of TAZ-overexpressing cells as compared with control counterpart. (**d**) *In vitro* migration ability of TAZ-depleted, TAZ-overexpressing cells and respective controls. Histogram quantifies relative migratory capacities. (**e**) Left: *in vivo* metastatic potential of the cell populations described above. Right: representative BLI image of metastatic colonization potential of BCSC LKO NT, BCSC LKO shTAZ, dBCC TWEEN and dBCC TWEEN TAZ. Data are the mean ± s.d. of three independent experiments in which three mice/group were employed.

whether TAZ expression is an independent prognostic factor that could be exploited for clinical use in BC. Thus, to assess whether our findings had clinical relevance, we determined TAZ expression by immunohistochemical staining in 99 consecutive BCs with complete follow-up data (Supplementary Table S3). Fifty-five percent stained positively for TAZ. No significant correlation was observed between TAZ positivity and standard pathological parameters such as tumor size ($P = 0.764$), lymph node status ($P = 0.149$), estrogen (ER; $P = 0.177$) and progesterone (PGR; $P = 0.219$) receptors (Supplementary Table S4). In contrast, TAZ expression positively correlated with high tumor grade ($P = 0.001$), HER2 overexpression ($P = 0.004$) and high Ki-67 proliferation index ($P = 0.008$) (Supplementary Table S4), thus confirming that TAZ expression may be associated with more aggressive biopathological parameters. Additionally, when our series of cases were analyzed by unadjusted Kaplan–Meier curves (Figure 6b), we observed that TAZ expression significantly affected disease-free survival (DFS) ($P = 0.014$). Patients with TAZ-positive

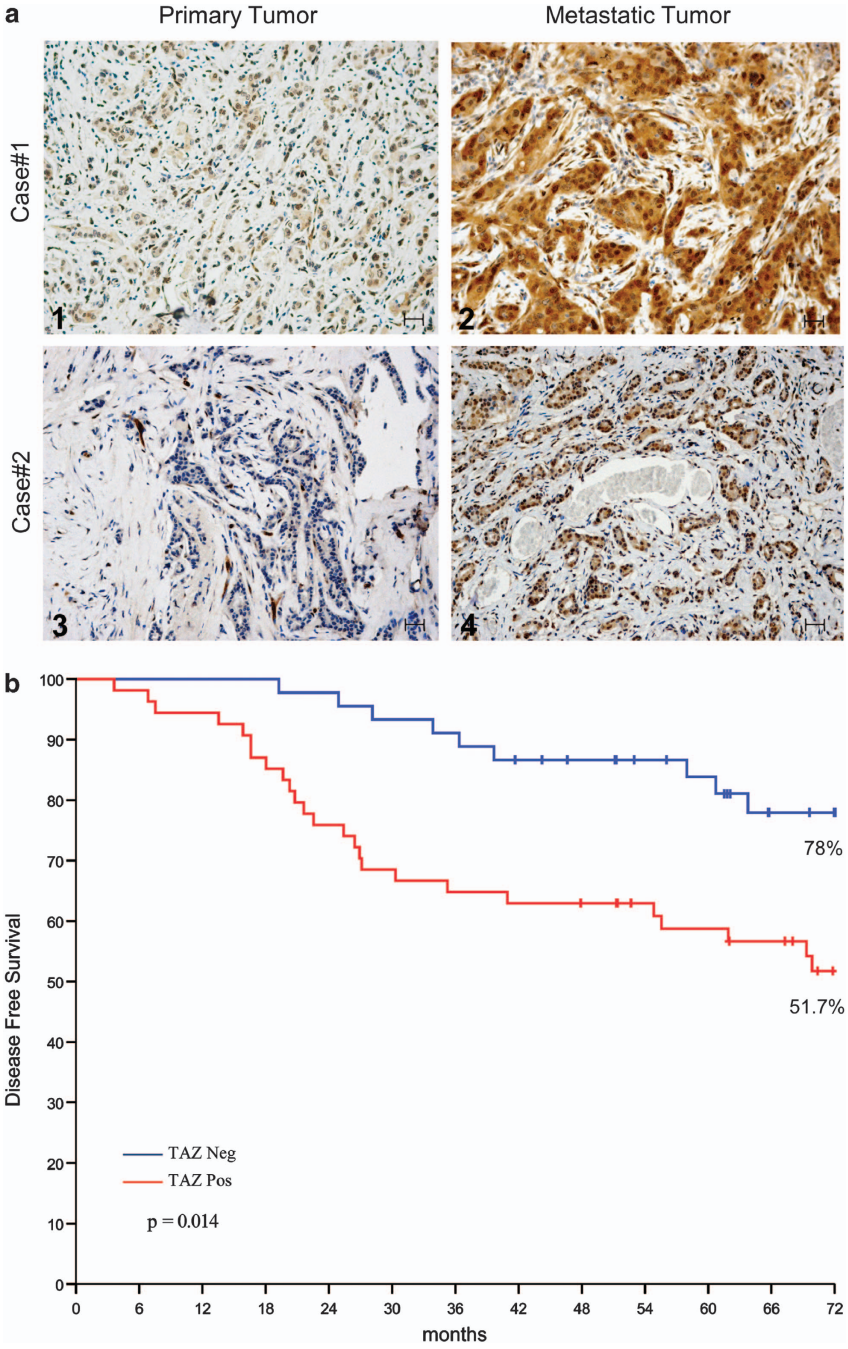

Figure 6. TAZ correlates with poor clinical outcome in human breast cancer patients. (**a**) Representative IHC pictures for TAZ expression in: G3 (panel 1) and G2 (panel 3) invasive human BC samples and corresponding matched lung metastases (panel 2 and 4) showing an increase in TAZ expression from score 1+ to score 3+ and 2+, respectively. Acquisition was made with a ×20 objective. (**b**) Kaplan–Meier curve representing DFS of patients with breast cancer stratified according to TAZ expression status. DFS was calculated from the date of tumor diagnosis to the date of first recurrence, including local relapses or distant metastases. *P*-values were calculated using the log-rank test.

tumors exhibited a shorter DFS (51.7% of cancer-free patients) than those with TAZ-negative BC (78% of cancer-free patients). As summarized in Table 2, the Cox univariate model highlighted that nodal status (hazard ratio (HR) 2.56, confidence interval (CI) 95%, 1.32–4.97, $P=0.005$), tumor grade (HR 0.44, CI 95%, 0.23–0.83, $P=0.011$) and TAZ positivity (HR 2.35, CI 95%, 1.16–4.77, $P=0.017$) significantly impact DFS. More importantly, multivariate analysis revealed that nodal status (HR 2.80, CI 95%, 1.40–5.60, $P=0.004$) and TAZ expression (HR 2.06, CI 95%, 1.01–4.20, $P=0.046$) were independent negative prognostic variables influencing DFS.

DISCUSSION

Understanding the molecular mechanisms responsible for chemoresistance and dissemination at secondary sites is critical for the successful treatment of BC. To date, several lines of evidence support the idea that CSCs contribute to both therapy resistance and metastatic dissemination.[25–29] However, to validate these ideas, progress must be made on the molecular mechanisms governing such processes, starting with the identification of genes and signals that define CSCs properties. The Hippo transducer TAZ has been shown to endow CSC properties to non-CSCs cells in BC cell lines.[10] Here, we developed preclinical models based on

patient-derived BCSCs to investigate the mechanisms underlying the hierarchical contribution of tumor cells in BC progression and chemoresistance. We found that TAZ has a key role in the aggressive behavior of BC and may represent a major determinant of the unfavorable clinical outcome in advanced BC patients.

Many experimental studies rely on the use of extensively cultured cell lines that may have lost the main features of cancer cells from the original tumors. We therefore generated patient-derived cultures enriched in BCSCs and developed an *in vivo* metastatic model that simulates the clinical course of BC patients, including the formation of primary tumors, surgery and subsequent metastatic spreading. This type of model showed that patient-derived BCSCs are the only population able to metastasize at distant organs, whereas dBCCs display a weak migratory activity and do not directly participate in the formation of metastases. Even though these findings partially confirm previous results,[30] this model provides a considerable tool to investigating different subpopulations of patient-derived tumor cells *in vivo*.

Recently, many attempts have been made for dissecting molecular signals associated with the onset of BC metastases. The introduction of high-throughput technologies broadened our knowledge on the genetic pathways associated with the development and progression of cancer.[31] Nevertheless, the relevance of a single pathway on BC metastatization is still unclear, especially when considered within the pyramidal organization of tumors. By taking advantage of gene expression profiling, we documented that the *in vivo* aggressiveness pattern (dBCCs < BCSCs) was correlated with the expression of TAZ, which ranked among the top most significantly overexpressed genes in the CSC compartment. In both normal and cancer cells, TAZ promotes proliferation, cell migration and invasion, whereas its expression correlates with the acquisition and maintenance of SC traits such as self-renewal and chemoresistance.[10,32,33] We found that, unlike in xenografts-derived dBCCs, TAZ is highly expressed and active in the BCSC counterparts and particularly in *in vivo* metastatic derivatives. Exogenous TAZ gain in dBCCs was associated with the acquisition of a mesenchymal-like phenotype, tumorigenic ability and increased cell motility.

Although previous work suggested a relationship between TAZ expression and poor patient outcome in BC patients,[10] a functional role of TAZ in tumor metastasis has never been reported before. Here, we show that the appearance of metastases was remarkably suppressed in TAZ-depleted BCSCs, even when these cells were injected in high number. In accordance with our experimental metastatic model, we detected increased TAZ levels in metastatic lesions as compared with matched primary tumors. Thus, it is likely that the involvement of TAZ in the metastatic spreading observed in our preclinical model recapitulates the events occurring in BC patients. Furthermore, we observed that high TAZ expression levels in patient tumors was an independent negative prognostic factor together with the presence of metastatic lymph nodes and negativity for estrogen receptors.

Table 1. TAZ expression in primary and paired metachronous metastatic BC

Total cases, N	*Primary breast cancer*	*Metastatic breast cancer*			
	TAZ score	*TAZ score*			
		0 (%)	*1+ (%)*	*2+ (%)*	*3+ (%)*
19	0	6 (32)	5 (26)	6 (32)	2 (10)
16	1+	0	5 (32)	9 (56)	2 (12)
17	2+	1 (6)	0	12 (71)	4 (23)
4	3+	0	0	0	4 (100)
56		7 (13)	10 (18)	27 (48)	12 (21)

TAZ was considered as positive when over 10% of tumor cells displayed nuclear TAZ immunostaining similar to (score 1+) or stronger (score 2+/3+) as compared with normal ducts cells included in the same section.

Table 2. Uni- and multivariate analyses

Factors	*Univariate analysis*		*Multivariate analysis*	
Patients n. 99	*HR (95% CI)*	P-*value*	*HR (95% CI)*	P-*value*
Tumor size				
T2-T4 vs T1	1.83 (0.97–3.47)	0.062		
Lymph node status				
Positive vs negative	2.56 (1.32–4.97)	0.005	2.80 (1.40–5.60)	0.004
Grading				
G1-G2 vs G3	0.44 (0.23–0.83)	0.011		
ER				
Positive vs negative	0.55 (0.27–1.12)	0.099	0.45 (0.22–0.95)	0.037
PgR				
Positive vs negative	0.60 (0.32–1.14)	0.121		
HER2				
Positive vs negative	1.23 (0.58–2.60)	0.596		
Ki-67				
High vs low	1.76 (0.90–3.45)	0.097		
TAZ				
Positive vs negative	2.35 (1.16–4.77)	0.017	2.06 (1.01–4.20)	0.046

Abbreviations: CI, confidence interval; HR, hazard ratio. ER/PgR: negative: <10; positive ≥10; HER2 negative: 0/1+/2+non amplified; HER2 positive: 2+amplified/3+; KI67 low: ≤15; high: >15.

Thus, these data complement and add greater clinical relevance to previous studies[10] by showing that TAZ is overexpressed in high-grade BC, correlates with overt metastatic lesions in human patients and is instrumental to incite metastasis in gain- and loss-of-function assays in mouse models.

Another relevant activity of TAZ in BCSCs concerns the protection from chemotherapy. Although TAZ does not confer chemoresistance to dBCCs, TAZ depletion sensitized BCSCs and relative tumor xenografts to chemotherapeutic drugs, suggesting that the presence of TAZ in BCSCs contributes significantly to drug resistance in BC. It has been speculated that the biological plasticity of CSCs may facilitate their survival in a secondary site. Intriguingly, this and previous studies indicate a scenario in which the morphological plasticity promoted by EMT (or just loss of apico-basal polarity) induced TAZ stabilization and, in turn, acquisition of CSC, drug resistance and metastatic properties. Future studies are required to identify the downstream targets through which TAZ induces distinct CSCs properties.

Because the understanding of the biological relevance in cancer of the Hippo pathway is very recent and rare germinal or somatic mutations have been described, there are no current drugs now under development targeting TAZ. However, we believe that TAZ warrants further clinical investigation in BC, holding the potential to implement the current pipeline of biomarkers and therapeutic targets.

MATERIALS AND METHODS

Isolation and cell cultures

BC specimens were obtained upon informed consent from patients undergoing surgical resection according to the Institutional Ethical Committee guidelines on human experimentation and the Declaration of Helsinki. Following surgical specimen dissociation, recovered cells were cultured in serum-free mediums as previously described.[13–15] To obtain differentiated BC cells (dBCCs), dissociated BCSCs were plated on collagen-coated plates for 48 h. A layer of Matrigel (BD Biosciences, San Jose, CA, USA) was subsequently added and cells were grown in complete mammary epithelial cell growth medium (Lonza, Allendale, NJ, USA).

Colony-forming ability assay

Soft agar colony-forming assays were carried out for untreated BCSCs and dBCCs as previously described.[34]

In vivo studies

Animal studies were performed according to the Istituto Superiore di Sanità guidelines on animal care under the Italian Ministry of Health authorization (D.M. n. 224/2011). BCSCs and dBCCs were suspended in 50 μl mixed 1:1 with Matrigel (BD Biosciences) and orthotopically injected into the left and right cleared fat pad of a 6-week-old NOD SCID IL-2Rnull (NSG) mice (Charles River Laboratories, Wilmington, MA, USA) together with HS-27A stromal cells (at 2:1 ratio) to humanize the mammary gland. To assess serial transplantation studies, tumor xenografts derived from distinct patient-derived BCSC lines were dissociated and 5×10^4 cells re-injected each time into the mammary fat pad of the 6-week-old NSG mice. For *in vivo* tracking, cells were transfected with lentiviral vector encoding luciferase/enhanced green fluorescent protein (Luc/EGFP-BCSCs) or luciferase/red fluorescent protein (Luc/RFP-dBCCs) reporter genes and a total of 10^4 cells were injected either intracardially or orthotopically, alone or in defined ratios (1:1). Bioluminescence imaging was used to assess primary tumor growth and the onset of distant metastases. A cryogenically cooled imaging system (IVIS 100 Imaging System, Xenogen, Alameda, CA, USA) was employed for whole body imaging following luciferin (100 mg/kg, Caliper Life Science, Hopkinton, MA, USA) administration. Signal intensities were quantified as the sum of all detected photons (Living Image Software 2.50, PerkinElmer, Hopkinton, MA, USA). To discriminate RFP-positive and EGFP-positive cells in tumor metastases, explanted organs were analyzed under an Olympus SZX10 stereomicroscope equipped with a fluorescence unit. For chemoresistance studies, doxorubicin was intraperitoneally administered 2 mg/kg twice a week for 2 weeks. Tumor growth was measured by an electronic caliper or evaluated through bioluminescence imaging.

Cell viability assays

For cell viability studies, 3×10^3 cells/well were seeded in 96-well plates. Doxorubicin (15 ng/ml) or paclitaxel (5 ng/ml), both from Sigma-Aldrich (St Louis, MO, USA), were used to evaluate sensitivity to chemotherapy. Cell viability was evaluated after 48 h as previously described.[34]

Migration assay

Cell migration was assessed in 24-well transwell boyden chambers (Costar Scientific Corporation, Cambridge, MA, USA). Single cells (2×10^4) were suspended in a complete growth medium and placed into upper chambers. After 24 h of incubation, migrated cells were stained with Coomassie Brilliant Blue and counted under the microscope.

Flow cytometry

For cell sorting of EGFP and RFP tumor cell populations, single-cell suspensions from primary and metastatic xenografts were collected and sorted with a FACS Aria (Becton Dickinson, Franklin Lakes, NJ, USA).

Immunofluorescence

For TAZ localization, FPS, FPD and MDA-MB-231 were permeabilized before incubation with 10 μg/ml mouse anti-TAZ (BD Bioscences). Alexa Fluor 488 and Alexa Fluor 555 (Molecular Probes/Invitrogen, Carlsbad, CA, USA) were used at 1 μg/ml as secondary antibodies. DAPI (Invitrogen) and Phalloidin-Alexa Fluor 647 (Molecular Probes/Invitrogen) were used at 1 μg/ml to visualize nuclei and F-actin cytoskeleton, respectively. Confocal images were obtained with an Olympus FV-1000 spectral confocal microscope equipped with an UltraPlan Fluorite 40 NA 1.3 objectives and the software Olympus Fluoview (Olympus, Tokyo, Japan).

Gene expression profiling

Gene array was performed as previously described.[35] Briefly, 100 ng of total RNA was labeled and hybridized to the Affymetrix GeneChip1.0ST array (Affymetrix, Santa Clara, CA, USA) following the manufacturer's instructions. Data analyses were performed by comparing tool classes of BRB-ArrayTools.

Western blot

For western blot analysis, 20 μg of whole-cell lysates were used. Nitrocellulose membranes were incubated with: anti-YAP/TAZ (D24E4) and β-actin, (Cell Signaling Technology, Danvers, MA, USA), or Nucleolin (Santa Cruz Biotechnology, Santa Cruz, CA, USA).

Lentiviral transduction

One cycle of infection with lentiviral supernatants Luc-EGFP and Luc-RFP was carried out on BCSCs and/or dBCCs culture. EGFP- and RFP-positive cells were isolated using a FACS Aria. For TAZ overexpression, TAZ cDNA was cloned into the lentiviral vector pRRL-CMV-PGK-EGFP-WPRE called TWEEN.[36] Two cycles of viral infection (with TWEEN and TWEEN TAZ supernatants) were performed on Luc/RFP-dBCCs. Lentiviral constructs LKO NT and LKO shTAZ were obtained as described.[10] Selection was carried out by exposition to puromycine 10 μg/ml (Sigma-Aldrich).

Immunohistochemistry

Immunohistochemistry on xenograft sections was performed on formalin-fixed, paraffin-embedded tissues. Paraffin sections (3 μm) were treated as previously described[34] and incubated with anti low and medium molecular weight cytokeratins (CKs, Dako, Fort Collins, CO, USA) and with the monoclonal antibody anti-TAZ (M2-616, BD Pharmingen, San Jose, CA, USA). For clinical data, formalin-fixed, paraffin-embedded sections were incubated with anti-ER (6F11, Leica, Milano, Italy), -PgR (1A6, Leica), -HER2 (A0485, Dako), -Ki-67 (MIB-1, Dako) and -TAZ. Immunostaining was performed using a pH6 antigen retrieval buffer in an automated autostainer (Bond Max, Menarini Diagnostic srl, Firenze, Italy).

Patients and scoring criteria

A retrospective series of 56 BC patients with matched metachronous metastases were selected to study TAZ modulation during disease progression. A series of 99 consecutive BC patients with a median follow-up of 92 months (CI: 95%; 3.61–126.49) were further investigated

according to the Ethics Committee of the Regina Elena National Cancer Institute to evaluate the prognostic role of TAZ expression. TAZ was considered positive when over 10% of tumor cells displayed nuclear TAZ immunostaining similar to (score 1+) or stronger (score 2+/3+) as compared with normal ducts cells included in the same section. HER2 was negative with a score (0 and 1+), equivocal (2+; to be confirmed by FISH), or positive (3+). ER and PgR were considered positive when >10% of the neoplastic cells showed distinct nuclear immunoreactivity. Ki-67 was regarded high if >15% of the cell nuclei were immunostained.

Statistical analysis

For *in vitro* and *in vivo* studies statistical analyses were performed using GraphPad Prism version 4 (www.graphpad.com). Statistical significance was determined by two-way analysis of variance with Bonferroni post-test. P value <0.05*, P value <0.01**, $P<0.001$***. Statistical analyses for clinical data were carried out using SPSS software (SPSS version 20.0, SPSS Inc., Chicago, IL, USA). The DFS curves were estimated by the Kaplan–Meier method starting from the date of tumor diagnosis to the date of first recurrence. Log-rank test was used to compare survival curves. The HR and the 95% CI were evaluated for each variable using the Cox univariate model. A multivariate Cox proportional hazard model was also developed using stepwise regression (forward selection) with predictive variables that were significant in the univariate analyses. The enter and remove limits were $P=0.10$ and $P=0.15$, respectively.

CONFLICT OF INTEREST

The authors declare no conflict of interest.

ACKNOWLEDGEMENTS

We thank Associazione Italiana Ricerca sul Cancro (AIRC) grants IG-10254 (MT) and IG 13431 (RDM) for financial support. We are grateful to Giuseppe Loreto for figure editing, Michele Signore and Mario Falchi for confocal acquisitions.

REFERENCES

1 Ferlay J, Shin HR, Bray F, Forman D, Mathers C, Parkin DM. Estimates of worldwide burden of cancer in 2008: GLOBOCAN 2008. *Int J Cancer* 2010; **127**: 2893–2917.
2 Saini V, Shoemaker RH. Potential for therapeutic targeting of tumor stem cells. *Cancer Sci* 2010; **101**: 16–21.
3 Kakarala M, Wicha MS. Implications of the cancer stem-cell hypothesis for breast cancer prevention and therapy. *J Clin Oncol* 2008; **26**: 2813–2820.
4 Maugeri-Sacca M, Vigneri P, De Maria R. Cancer stem cells and chemosensitivity. *Clin Cancer Res* 2011; **17**: 4942–4947.
5 Zhou BB, Zhang H, Damelin M, Geles KG, Grindley JC, Dirks PB. Tumour-initiating cells: challenges and opportunities for anticancer drug discovery. *Nat Rev Drug Discov* 2009; **8**: 806–823.
6 Schatton T, Murphy GF, Frank NY, Yamaura K, Waaga-Gasser AM, Gasser M *et al.* Identification of cells initiating human melanomas. *Nature* 2008; **451**: 345–349.
7 Malanchi I, Santamaria-Martinez A, Susanto E, Peng H, Lehr HA, Delaloye JF *et al.* Interactions between cancer stem cells and their niche govern metastatic colonization. *Nature* 2012; **481**: 85–89.
8 Baccelli I, Schneeweiss A, Riethdorf S, Stenzinger A, Schillert A, Vogel V *et al.* Identification of a population of blood circulating tumor cells from breast cancer patients that initiates metastasis in a xenograft assay. *Nat Biotechnol* 2013; **31**: 539–544.
9 Harvey KF, Zhang X, Thomas DM. The Hippo pathway and human cancer. *Nat Rev Cancer* 2013; **13**: 246–257.
10 Cordenonsi M, Zanconato F, Azzolin L, Forcato M, Rosato A, Frasson C *et al.* The Hippo transducer TAZ confers cancer stem cell-related traits on breast cancer cells. *Cell* 2011; **147**: 759–772.
11 Mani SA, Guo W, Liao MJ, Eaton EN, Ayyanan A, Zhou AY *et al.* The epithelial-mesenchymal transition generates cells with properties of stem cells. *Cell* 2008; **133**: 704–715.
12 Perrone G, Gaeta LM, Zagami M, Nasorri F, Coppola R, Borzomati D *et al. In situ* identification of CD44+/CD24- cancer cells in primary human breast carcinomas. *PLoS One* 2012; **7**: e43110.
13 Ricci-Vitiani L, Lombardi DG, Pilozzi E, Biffoni M, Todaro M, Peschle C *et al.* Identification and expansion of human colon-cancer-initiating cells. *Nature* 2007; **445**: 111–115.
14 Eramo A, Lotti F, Sette G, Pilozzi E, Biffoni M, Di Virgilio A *et al.* Identification and expansion of the tumorigenic lung cancer stem cell population. *Cell Death Differ* 2008; **15**: 504–514.
15 Ponti D, Costa A, Zaffaroni N, Pratesi G, Petrangolini G, Coradini D *et al.* Isolation and *in vitro* propagation of tumorigenic breast cancer cells with stem/progenitor cell properties. *Cancer Res* 2005; **65**: 5506–5511.
16 Grefte S, Vullinghs S, Kuijpers-Jagtman AM, Torensma R, Von den Hoff JW. Matrigel but not collagen I, maintains the differentiation capacity of muscle derived cells *in vitro*. *Biomed Mater* 2012; **7**: 055004.
17 Dontu G, Abdallah WM, Foley JM, Jackson KW, Clarke MF, Kawamura MJ *et al. In vitro* propagation and transcriptional profiling of human mammary stem/progenitor cells. *Genes Dev* 2003; **17**: 1253–1270.
18 Zhao B, Lei QY, Guan KL. The Hippo-YAP pathway: new connections between regulation of organ size and cancer. *Curr Opin Cell Biol* 2008; **20**: 638–646.
19 Lladser A, Sanhueza C, Kiessling R, Quest AF. Is survivin the potential Achilles' heel of cancer? *Adv Cancer Res* 2011; **111**: 1–37.
20 Yin D, Chen W, O'Kelly J, Lu D, Ham M, Doan NB *et al.* Connective tissue growth factor associated with oncogenic activities and drug resistance in glioblastoma multiforme. *Int J Cancer* 2010; **127**: 2257–2267.
21 Chaffer CL, Weinberg RA. A perspective on cancer cell metastasis. *Science* 2011; **331**: 1559–1564.
22 Gonzalez-Angulo AM, Morales-Vasquez F, Hortobagyi GN. Overview of resistance to systemic therapy in patients with breast cancer. *Adv Exp Med Biol* 2007; **608**: 1–22.
23 Morris PG, McArthur HL, Hudis CA. Therapeutic options for metastatic breast cancer. *Expert Opin Pharmacother* 2009; **10**: 967–981.
24 Lai D, Ho KC, Hao Y, Yang X. Taxol resistance in breast cancer cells is mediated by the hippo pathway component TAZ and its downstream transcriptional targets Cyr61 and CTGF. *Cancer Res* 2011; **71**: 2728–2738.
25 Abraham BK, Fritz P, McClellan M, Hauptvogel P, Athelogou M, Brauch H. Prevalence of CD44+/CD24-/low cells in breast cancer may not be associated with clinical outcome but may favor distant metastasis. *Clin Cancer Res* 2005; **11**: 1154–1159.
26 Aktas B, Tewes M, Fehm T, Hauch S, Kimmig R, Kasimir-Bauer S. Stem cell and epithelial-mesenchymal transition markers are frequently overexpressed in circulating tumor cells of metastatic breast cancer patients. *Breast Cancer Res* 2009; **11**: R46.
27 Theodoropoulos PA, Polioudaki H, Agelaki S, Kallergi G, Saridaki Z, Mavroudis D *et al.* Circulating tumor cells with a putative stem cell phenotype in peripheral blood of patients with breast cancer. *Cancer Lett* 2010; **288**: 99–106.
28 Balic M, Lin H, Young L, Hawes D, Giuliano A, McNamara G *et al.* Most early disseminated cancer cells detected in bone marrow of breast cancer patients have a putative breast cancer stem cell phenotype. *Clin Cancer Res* 2006; **12**: 5615–5621.
29 Liu R, Wang X, Chen GY, Dalerba P, Gurney A, Hoey T *et al.* The prognostic role of a gene signature from tumorigenic breast-cancer cells. *New Engl J Med* 2007; **356**: 217–226.
30 D'Amico L, Patane S, Grange C, Bussolati B, Isella C, Fontani L *et al.* Primary breast cancer stem-like cells metastasise to bone, switch phenotype and acquire a bone tropism signature. *Br J Cancer* 2013; **108**: 2525–2536.
31 Cardoso F, Van't Veer L, Rutgers E, Loi S, Mook S, Piccart-Gebhart MJ. Clinical application of the 70-gene profile: the MINDACT trial. *J Clin Oncol* 2008; **26**: 729–735.
32 Lei QY, Zhang H, Zhao B, Zha ZY, Bai F, Pei XH *et al.* TAZ promotes cell proliferation and epithelial-mesenchymal transition and is inhibited by the hippo pathway. *Mol Cell Biol* 2008; **28**: 2426–2436.
33 Chan SW, Lim CJ, Guo K, Ng CP, Lee I, Hunziker W *et al.* A role for TAZ in migration, invasion, and tumorigenesis of breast cancer cells. *Cancer Res* 2008; **68**: 2592–2598.
34 Bartucci M, Svensson S, Romania P, Dattilo R, Patrizii M, Signore M *et al.* Therapeutic targeting of Chk1 in NSCLC stem cells during chemotherapy. *Cell Death Differ* 2012; **19**: 768–778.
35 Pagliuca A, Valvo C, Fabrizi E, di Martino S, Biffoni M, Runci D *et al.* Analysis of the combined action of miR-143 and miR-145 on oncogenic pathways in colorectal cancer cells reveals a coordinate program of gene repression. *Oncogene* 2012; **32**: 4806–4813.
36 Bonci D, Cittadini A, Latronico MV, Borello U, Aycock JK, Drusco A *et al.* 'Advanced' generation lentiviruses as efficient vectors for cardiomyocyte gene transduction *in vitro* and *in vivo*. *Gene Ther* 2003; **10**: 630–636.

Supplementary Information accompanies this paper on the Oncogene website (http://www.nature.com/onc)